Journal of Alloys and Compounds 509 (2011) 6889–6892

Contents lists available at ScienceDirect

Journal of Alloys and Compounds

journal homepage: www.elsevier.com/locate/jallcom

Magnetic properties and large magnetocaloric effect in Gd–Ni amorphous ribbons for magnetic refrigeration applications in intermediate temperature range

X.C. Zhong[a,*], P.F. Tang[a], Z.W. Liu[a], D.C. Zeng[a], Z.G. Zheng[a], H.Y. Yu[a], W.Q. Qiu[a], M. Zou[b,1]

[a] School of Materials Science and Engineering, South China University of Technology, Guangzhou 510640, China
[b] Ames Laboratory, U.S. Department of Energy, Iowa State University, Ames, IA 50011-3020, USA

ARTICLE INFO

Article history:
Received 11 December 2010
Received in revised form 30 March 2011
Accepted 30 March 2011
Available online 7 April 2011

Keywords:
Gd–Ni amorphous alloys
Melt spinning
Magnetocaloric effect
Magnetic refrigeration

ABSTRACT

Amorphous $Gd_{68-x}Ni_{32+x}$ ($x = -3$, 0, 3) ribbons were prepared by melt-spinning method. The crystallization onset temperatures T_{x1} for $Gd_{68-x}Ni_{32+x}$ amorphous ribbons with $x = -3$, 0, and 3 are 561, 568, and 562 K, respectively. All the samples undergo the second-order magnetic transition at temperatures between ~122 ($x = -3$ and 3) and 124 K ($x = 0$). The Curie temperature T_C does not change with the composition significantly. The maximum isothermal magnetic entropy changes $(-\Delta S_M)_{max}$ of $Gd_{71}Ni_{29}$, $Gd_{68}Ni_{32}$, and $Gd_{65}Ni_{35}$ amorphous ribbons for a magnetic field change of 0–5 T were 9.0, 8.0, and 6.9 J kg^{-1} K^{-1}, respectively. Large values of the refrigerant capacity (RC) were obtained in these ribbons. For example, $Gd_{71}Ni_{29}$ amorphous ribbon has a maximum RC value of 724 J kg^{-1}. Large magnetic entropy change and RC values together with high stability enable the $Gd_{71}Ni_{29}$ amorphous alloy a competitive candidate among the magnetic refrigeration materials working at temperatures near 120 K.

1. Introduction

Compared with the traditional gas compression refrigeration, magnetic refrigeration has advantages such as high-efficiency, energy-conservation, and environment-friendliness [1], which can help reaching the goal of low carbon economy advocated in the modern world. Magnetic refrigeration is based on the magnetocaloric effect (MCE) of magnetic materials, which is characterized by their isothermal magnetic entropy change (ΔS_M). Large ΔS_M values have been reported in materials with first-order phase transitions, such as $Gd_5(Si_xGe_{1-x})_4$ [2], $La(Fe_{1-x}Si_x)_{13}$ [3,4], $MnFeP_{1-x}As_x$ [5], $MnAs_{1-x}Sb_x$ [6,7], and Ni–Mn-based alloys [8,9]. For magnetic refrigeration technology, refrigerant capacity (RC) is another important parameter for efficiency evaluation [10,11]. In order to get a large RC value, a broad range of magnetic phase transitions and a large ΔS_M value are needed. Although large ΔS_M values were found in the materials mentioned above, large thermal and magnetic hysteresis accompanied by the first order magnetic phase transition (FOMT) and narrow magnetic ordering range resulted in small RC values, which limit their practical application [9]. In contrast, materials with second order magnetic phase transitions (SOMT) have a wide range of magnetic ordering transition temperatures, although their ΔS_M is low, their RC value is relatively large [12,13]. For example, the value of the ΔS_M peak of the $Gd_5Ge_2Si_2$ alloy (a FOMT material) with an applied field change of $\Delta\mu_0 H = 5$ T is about 3 times of the $Gd_5Ge_{1.9}Si_2Fe_{0.1}$ alloy (a SOMT material) (20 J kg^{-1} K^{-1} versus 7 J kg^{-1} K^{-1}). However, the broader ΔS_M peak width of the $Gd_5Ge_{1.9}Si_2Fe_{0.1}$ alloy results in a greater RC value (360 J kg^{-1}) than that of the $Gd_5Ge_2Si_2$ alloy (305 J kg^{-1}) [13].

Soft magnetic amorphous alloys for magnetic refrigeration application have various advantages such as low magnetic and thermal hystereses, high electrical resistivity (which will lower eddy current heating arising from the varying magnetic field), weak coercive force, enhanced corrosion resistance, good mechanical properties, and adjustable Curie temperature (T_C) [14–16]. In addition, a wide range of magnetic ordering transition temperatures and a large RC value make this series of materials suitable for Ericsson refrigeration cycle and to be one of the most competitive types of refrigerants. At present, researches on amorphous magnetic refrigerants are mainly focused on heavy rare earth-based [14,17–21] and transition metal-based alloys [15,16,22–24].

Heavy rare earth (HRE) – transition metal (TM) binary alloys have large magnetic moments and complex magnetic structures [21,25–28]. The work by Liu et al. [28] on thermomagnetic properties of amorphous rare-earth metals alloyed with Fe, Ni, or Co revealed that the magnetic transitions in these alloys were significantly broadened. Zhang et al. [21] found that both ΔS_M and RC featured a large value in Gd–Co binary amorphous alloys. For

* Corresponding author. Tel.: +86 20 87111312; fax: +86 20 87111312.
E-mail address: xczhong@scut.edu.cn (X.C. Zhong).
[1] Current address: Ceramic and Metallurgy Technologies, GE Global Research Center, Niskayuna, NY 12309, USA.

0925-8388/$ – see front matter © 2011 Elsevier B.V. All rights reserved.
doi:10.1016/j.jallcom.2011.03.173

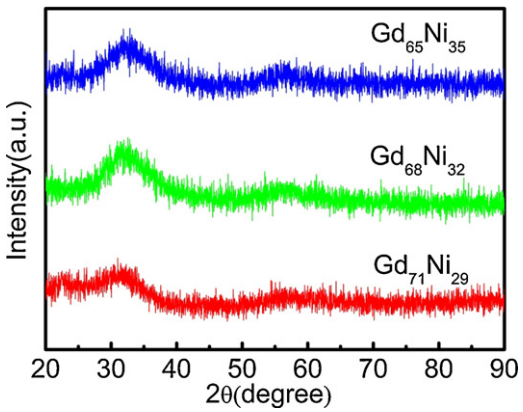

Fig. 1. X-ray diffraction patterns for melt-spun $Gd_{68-x}Ni_{32+x}$ ribbons.

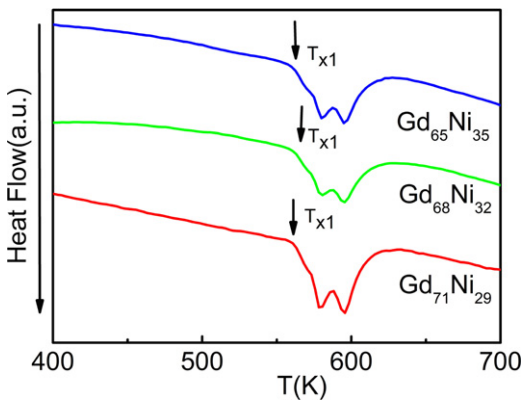

Fig. 3. DSC curves for $Gd_{68-x}Ni_{32+x}$ ribbons melt-spun at the speed of 60 m/s.

example, under an applied magnetic field of 1 T, ΔS_M and RC in $Gd_{71}Co_{29}$ alloy are 3.1 J kg^{-1} K^{-1} and 92.3 J kg^{-1}, respectively. It was also found that with the decrease in Gd/Co ratio (71:29, 68:32, 65:35 and 62:38), T_C of these alloys increase gradually from 166 to 193 K. Up to date, amorphous Gd–Ni alloys have not been well studied. Although most work on MCE focused on the materials with magnetic transition at room temperature, the MCE materials with different T_C have practical merits. For example, in order to reach the temperature below liquid H_2, we may employ two or three order pre-cooling technology, which operates at 300–200 K, 200–100 K, and 100–50 K. Therefore, in this paper, we report on the magnetic properties and magnetocaloric effects of $Gd_{68-x}Ni_{32+x}$ ($x = -3, 0, 3$) amorphous alloys. Similar to the Gd–Co alloy, the composition of $Gd_{68}Ni_{32}$ is located near the eutectic point on the Gd–Ni phase diagram [29]. Hence, it would be relatively easy to make these alloys amorphous.

2. Experimental details

Binary $Gd_{68-x}Ni_{32+x}$ ($x = -3, 0, 3$) ingots were prepared by arc melting a mixture of 99.9% pure Gd and Ni components in a Ti-gettered argon atmosphere. The ingots were re-melted four times to ensure compositional homogeneity. The crushed pieces of ingots were melt-spun into ribbons at a copper wheel having a surface speed of 60 m/s using a single-roller melt-spinner. X-ray diffraction (XRD) measurements were performed on a Philips diffractometer with Cu Kα_1 radiation. Differential scanning calorimetry (DSC) data were collected at a heating rate of 20 K/min. The crystallization onset temperature (T_{x1}) was defined by the intersection of the extrapolation of two tangents of the beginning inflection point at both ends of the linear part of the first exothermic peak of the DSC curve. Magnetic measurements were carried out on a Quantum Design Physical Property Measurement System (model PPMS-9) equipped with a 9 T vibrating sample magnetometer.

The magnetization (M) as a function of temperature (T) was measured with an applied magnetic field of 0.01 T. The Curie temperature (T_C) was defined as the temperature at the maximum of $|dM/dT|$ vs. T plot. From isothermal magnetization data, the magnetic entropy change was calculated by using the Maxwell relation $(\partial S/\partial H)_T = (\partial M/\partial T)_H$, where S, M, H, and T represent the magnetic entropy, magnetization, applied magnetic field, and temperature, respectively.

3. Results and discussion

The XRD patterns of the as-spun $Gd_{68-x}Ni_{32+x}$ ribbons are shown in Fig. 1. Only one broad hump appears between 2θ of 25° and 35°, and no well-defined diffraction peaks of crystalline phases are presented, indicating an amorphous structure of the as-spun ribbons.

The temperature dependencies of magnetization for the amorphous samples measured in an applied field of 0.01 T between 5 and 300 K under the zero-field cooling (ZFC) and field cooling (FC) conditions are shown in Fig. 2. The ZFC and the FC curves overlap each other in the whole temperature range. The small difference in Ni concentration has no significant effect on the magnetic ordering temperature. The Curie temperature T_C was determined to be 122, 124, and 122 K for $Gd_{68-x}Ni_{32+x}$ amorphous samples with $x = -3$, 0, and 3, respectively.

In the DSC curves (Fig. 3), two exothermic peaks appear in the temperature range between 540 and 600 K for all the $Gd_{68-x}Ni_{32+x}$ amorphous ribbons, corresponding to two crystallization transitions. A hump at the low temperature part of the first peak for all alloys, is attributed to the growth of primary nanocrystals prior to phase separation and primary crystallization [30]. The first and second exothermic peaks are likely due to secondary crystallization and the formation of high temperature crystalline phases, respectively. This conjecture was proved by the x-ray diffraction (XRD) measurements conducted on the samples which were heated to 650 K with DSC. The XRD patterns showed lines characteristic of two crystalline phases commonly observed in crystalline $Gd_{68}Ni_{32}$, namely the Gd_3Ni (Fe_3C structure type) and GdNi (BCr

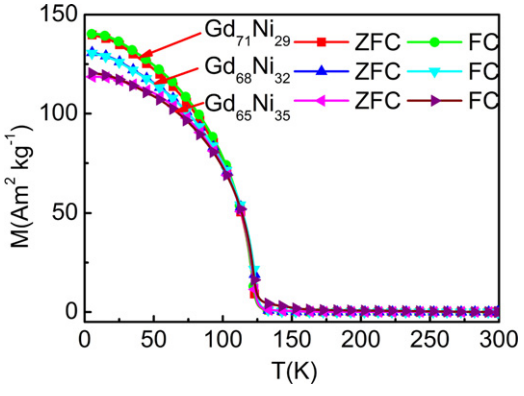

Fig. 2. Temperature dependence of magnetization for $Gd_{68-x}Ni_{32+x}$ melt-spun ribbons measured at a magnetic field of 0.01 T.

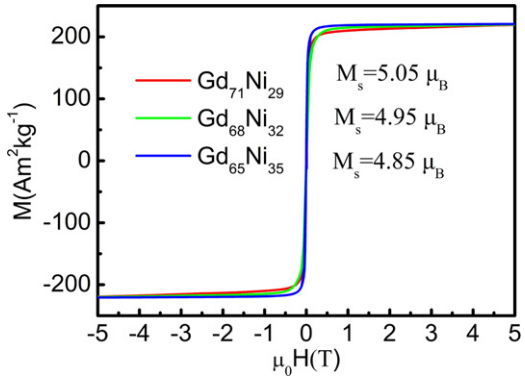

Fig. 4. Magnetization curves of $Gd_{68-x}Ni_{32+x}$ melt-spun ribbons measured at 5 K.

Table 1
Magnetocaloric properties of some typical magnetic refrigerants including amorphous and crystalline materials. A and C stand for amorphous and crystalline alloys, respectively.

Material	Structure	T_C (K)	$-\Delta S_M$ (J kg^{-1} K^{-1})	RC (J kg^{-1})	Applied field (T)	Reference
$Gd_{71}Ni_{29}$	A	122	9.0	724	5	This work
$Gd_{68}Ni_{32}$	A	124	8.0	583	5	This work
$Gd_{65}Ni_{35}$	A	122	6.9	524	5	This work
$Gd_{71}Co_{29}$	A	166	3.1	92	1	[21]
$Gd_5Ge_2Si_2$	C	275	20.0	305	5	[13]
$Gd_5Ge_{1.9}Si_2Fe_{0.1}$	C	305	7.0	360	5	[13]
Gd	C	293	9.7	556	5	[34]
$Gd_6Co_2Si_3$	C	295	6.3	503	5	[34]
$La(Fe_{0.88}Si_{0.12})_{13}$	C	195	23	452	5	[35]

structure type) structure types [29]. The crystallization onset temperatures T_{x1} of $Gd_{68-x}Ni_{32+x}$ amorphous ribbons with $x = -3$, 0, and 3 are 561, 568, and 562 K, respectively. It is well known that amorphous magnetic refrigerants are generally used in the vicinity of its magnetic ordering temperature. In these amorphous alloys, the crystallization onset temperatures are much higher than their magnetic ordering temperatures. Hence the $Gd_{68-x}Ni_{32+x}$ amorphous ribbons are stable in the range of practical application temperatures, which means that, from engineering point of view, amorphous $Gd_{68-x}Ni_{32+x}$ alloys have high temperature stability.

Fig. 4 shows the hysteresis loops of $Gd_{68-x}Ni_{32+x}$ amorphous alloys measured at 5 K. All alloys show negligible hysteresis and coercivity, which result from the zero orbital momentum of Gd atoms. The samples are magnetically saturated at 5 K in the applied field of 5 T and the saturation magnetization (M_s) is 219.3, 219.8 and 220.7 A m^2 kg^{-1}, which equal to 5.05, 4.95, and 4.85μ_B/magnetic atom, for $x = -3$, 0, and 3, respectively. Gd^{3+} is an *S*-state ion with negligible magnetic anisotropy, which was demonstrated by the essentially zero hysteresis and the small applied field needed for saturating the magnetization of the $Gd_{68-x}Ni_{32+x}$ alloys at low temperatures (Fig. 4). Also, Ni atoms do not carry a magnetic moment in the amorphous $Gd_{70}Ni_{30}$ alloy because the concentration of Ni is far below the critical concentration of 80 at.% for Ni to be magnetic in the RE-Ni alloys [31] and would not be expected to contribute to magnetic properties. Therefore, the magnetization of $Gd_{68-x}Ni_{32+x}$ alloys can be understood by assuming zero moment on Ni or a small moment on Ni coupled anti-parallelly to that of Gd. Antiferromagnetic coupling of the Gd and Ni moments occur in these amorphous alloys [28,32].

Isothermal magnetization $M(H)$ curves of the $Gd_{71}Ni_{29}$ amorphous ribbon are presented in Fig. 5(a). A typical ferromagnetic transition is evident in the vicinity of T_C. The Arrott plots of the $Gd_{71}Ni_{29}$ amorphous ribbon are displayed in Fig. 5(b). All slopes remain positive, indicating the ferromagnetic–paramagnetic transition is of second-order [33].

Isothermal magnetic entropy changes ($-\Delta S_M$) of these amorphous ribbons were calculated based on the magnetization isotherms in the vicinity of T_C by using the Maxwell relation. Fig. 6 shows the temperature dependence of the ($-\Delta S_M$) with different magnetic field changes. For the applied field change from 0 to 5 T, the maximum ($-\Delta S_M$) for $Gd_{71}Ni_{29}$, $Gd_{68}Ni_{32}$ and $Gd_{65}Ni_{35}$ amorphous ribbons are 9.0, 8.0, and 6.9 J kg^{-1} K^{-1}, respectively. The ($-\Delta S_M$) vs. T curves displays typical λ-shape, as shown usually in magnetic materials with a second-order magnetic transition, indicating that magnetic phase transition near Curie temperature of $Gd_{68-x}Ni_{32+x}$ amorphous alloys is second-order phase transition, which is in good agreement with the results of Arrott plots. The RC values of these amorphous ribbons were calculated by numerically integrating the area under

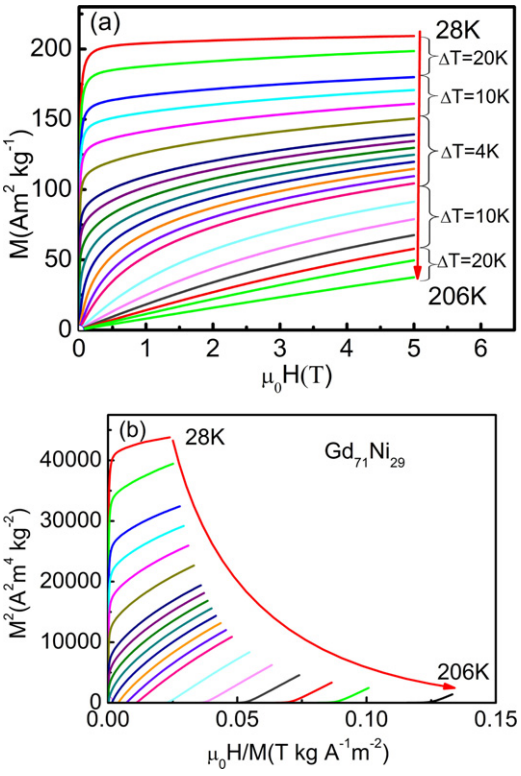

Fig. 5. (a) Magnetization isotherms of $Gd_{71}Ni_{29}$ melt-spun ribbon. The temperature was changed in steps of 4 K in the vicinity of T_C, and it was in 10–20 K steps for temperature further away from T_C. (b) Arrott plots of $Gd_{71}Ni_{29}$ melt-spun ribbon constructed from $M(H)$ data.

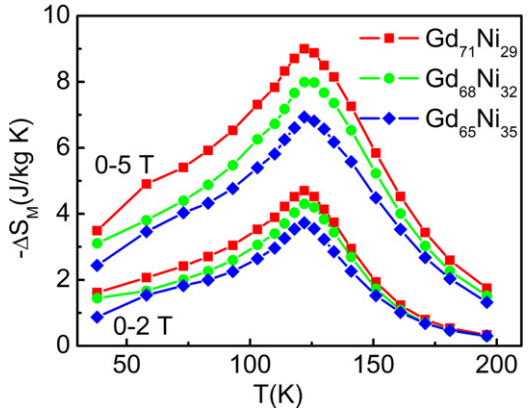

Fig. 6. Temperature dependence of magnetic entropy changes ($-\Delta S_M$) of $Gd_{68-x}Ni_{32+x}$ melt-spun ribbons for the magnetic field changes from 0 to 2 T and 5 T, respectively.

the $(-\Delta S_M)$ vs. T curves, using the temperatures at half maximum of the peak as the integration limits [11,13]. When the applied field changed from 0 to 5 T, RC values of $Gd_{71}Ni_{29}$, $Gd_{68}Ni_{32}$, and $Gd_{65}Ni_{35}$ amorphous ribbons were 724, 583, and 524 J kg^{-1}, respectively. These values are larger than that of Gd (556 J kg^{-1}, $\Delta\mu_0 H = 5.0$ T) [34] and $Gd_5Si_2Ge_2$ (305 J kg^{-1}, $\Delta\mu_0 H = 5.0$ T) [13]. The RC values of a series of magnetic refrigeration materials are listed in Table 1. For Gd–Ni amorphous ribbons, the structure disorder results in exchange integral fluctuation, which brings a wide range of magnetic ordering transition temperatures [28]. Therefore, the RC values of Gd–Ni amorphous ribbons are relatively large.

4. Conclusions

$Gd_{68-x}Ni_{32+x}$ ($x = -3, 0, 3$) amorphous ribbons were prepared by melt spinning with a wheel surface speed of 60 m/s. All these amorphous ribbons order ferromagnetically and undergo second-order transitions at their Curie temperatures. The composition change has negligible effect on the Curie temperatures of $Gd_{68-x}Ni_{32+x}$ amorphous ribbons. These amorphous ribbons have large values of ΔS_M and RC. The maximum isothermal magnetic entropy change $(-\Delta S_M)_{max}$ and RC value of $Gd_{71}Ni_{29}$ amorphous ribbons were 9.0 J kg^{-1} K^{-1} and 724 J kg^{-1}, respectively. Negligible coercive force and hysteresis, and large ΔS_M and RC values suggest that $Gd_{68-x}Ni_{32+x}$ amorphous ribbons are good candidates for active magnetic refrigeration working at temperatures around 120 K.

Acknowledgements

This work was financially supported by the Guangdong Provincial Science and Technology Program (Grant Nos. 2010B050300008, 2009B090300273 and 2007B010600043) and the Fundamental Research Funds for the Central Universities, SCUT (Grant No. 2009ZM0291). M. Zou's work was performed at Ames Laboratory, which was supported by the Office of Basic Energy Sciences, Materials Sciences Division of the Office of Science. The Ames Laboratory is operated by Iowa State University of Science and Technology for the U.S. Department of Energy under contract No. DE-AC02-07CH11358.

References

[1] K.A. Gschneidner Jr., V.K. Pecharsky, A.O. Tsokol, Rep. Prog. Phys. 68 (2005) 1479.
[2] V.K. Pecharsky, K.A. Gschneidner Jr., Phys. Rev. Lett. 78 (1997) 4494.
[3] F.X. Hu, B.G. Shen, J.R. Sun, Z.H. Cheng, G.H. Rao, X.X. Zhang, Appl. Phys. Lett. 78 (2001) 3675.
[4] S.J. Kim, K.J. Lee, M.H. Jung, H.J. Oh, Y.S. Kwon, J. Magn. Magn. Mater. 323 (2011) 1094.
[5] O. Tegus, E. Brück, K.H.J. Buschow, F.R. de Boer, Nature (London) 415 (2002) 150.
[6] H. Wada, Y. Tanabe, Appl. Phys. Lett. 79 (2001) 3302.
[7] L.G. de Medeiros Jr., N.A. de Oliveira, A. Troper, J. Alloys Compd. 501 (2010) 177.
[8] I. Dincer, E. Yüzüak, Y. Elerman, J. Alloys Compd. 509 (2011) 794.
[9] S.C. Ma, Q.Q. Cao, H.C. Xuan, C.L. Zhang, L.J. Shen, D.H. Wang, Y.W. Du, J. Alloys Compd. 509 (2011) 1111.
[10] M.E. Wood, W.H. Potter, Cryogenics 25 (1985) 667.
[11] K.A. Gschneidner Jr., V.K. Pecharsky, A.O. Pecharsky, C.B. Zimm, Mater. Sci. Forum 315 (1999) 69.
[12] D.H. Wang, S.L. Huang, Z.D. Han, Z.H. Su, W.Q. Zou, Y.W. Du, J. Alloys Compd. 377 (2004) 72.
[13] V. Provenzano, A.J. Shapiro, R.D. Shull, Nature (London) 429 (2004) 853.
[14] Q.Y. Dong, B.G. Shen, J. Chen, J. Shen, F. Wang, H.W. Zhang, J.R. Sun, J. Appl. Phys. 105 (2009) 053908.
[15] J.Y. Law, R.V. Ramanujan, V. Franco, J. Alloys Compd. 508 (2010) 14.
[16] P. Álvarez, J. Sánchez Marcos, P. Gorria, L. Fernández Barquín, J.A. Blanco, J. Alloys Compd. 504S (2010) S150.
[17] Z.Y. Xu, X. Hui, E.R. Wang, J. Chang, G.L. Chen, J. Alloys Compd. 504 (2010) 146.
[18] Q. Luo, W.H. Wang, J. Alloys Compd. 495 (2010) 209.
[19] J. Du, Q. Zheng, Y.B. Li, Q. Zhang, D. Li, Z.D. Zhang, J. Appl. Phys. 103 (2008) 023918.
[20] Q. Luo, D.Q. Zhao, M.X. Pan, W.H. Wang, Appl. Phys. Lett. 89 (2006) 081914.
[21] C.L. Zhang, D.H. Wang, Z.D. Han, H.C. Xuan, B.X. Gu, Y.W. Du, J. Appl. Phys. 105 (2009) 013912.
[22] Y.Y. Wang, X.F. Bi, Appl. Phys. Lett. 95 (2009) 262501.
[23] Y.K. Fang, C.C. Yeh, C.C. Hsieh, C.W. Chang, H.W. Chang, W.C. Chang, X.M. Li, W. Li, J. Appl. Phys. 105 (2009) 07A910.
[24] R. Caballero-Flores, V. Franco, A. Conde, K.E. Knipling, M.A. Willard, Appl. Phys. Lett. 96 (2010) 182506.
[25] P.J. von Ranke, D.F. Grangeia, A. Caldas, N.A. de Oliveira, J. Appl. Phys. 93 (2003) 4055.
[26] K. Pramod, K.G. Suresh, A.K. Nigam, O. Gutfleisch, J. Phys. D: Appl. Phys. 41 (2008) 245006.
[27] X.B. Liu, Z. Altounian, J. Appl. Phys. 107 (2010) 09E117.
[28] X.Y. Liu, J.A. Barclay, R.B. Gopal, M. Foldeaki, R. Chahine, T.K. Bose, P.J. Schurer, J.L. LaCombe, J. Appl. Phys. 79 (1996) 1630.
[29] Y.Y. Pan, C.S. Cheng, M. Li, H. Yang, Acta Phys. Sin. (China) 35 (1986) 677.
[30] C.C. Hays, C.P. Kim, W.L. Johnson, Appl. Phys. Lett. 75 (1999) 1089.
[31] A. Lienard, J.P. Rebouillat, J. Appl. Phys. 49 (1978) 1680.
[32] T.R. McGuire, R.J. Gambino, IEEE Trans. Magn. 14 (1978) 838.
[33] J.S. Kouvel, M.E. Fisher, Phys. Rev. 136 (1964) A1626.
[34] J. Shen, J.F. Wu, J.R. Sun, J. Appl. Phys. 106 (2009) 083902.
[35] A. Fujita, K. Fukamichi, J. Alloys Compd. 404–406 (2005) 554.